

Photon-excited soft-x-ray emission from LiBr and LiCl: Phonon relaxation for Li *K* excitations

K. E. Miyano* and D. L. Ederer

Tulane University, New Orleans, Louisiana 70118

T. A. Callcott, Q.-Y. Dong, J. J. Jia, and L. Zhou

University of Tennessee, Knoxville, Tennessee 37996

D. R. Mueller

National Institute of Standards and Technology, Gaithersburg, Maryland 20899

(Received 8 July 1993; revised manuscript received 29 October 1993)

Li *K* soft-x-ray emission spectra excited with monochromatic synchrotron radiation have been measured for LiBr and LiCl. The white-light reflectivity of these samples has also been recorded as a measurement of the Li *K* excitation spectra. The phonon relaxations involved in Li *K* excitations to the conduction band were determined to be 1.0 and 1.2 eV in the LiBr and LiCl, respectively, based on the energies of the valence band maxima in the x-ray emission spectra and their comparison to the energies of the valence band maxima and the Li *1s* core levels as measured by photoemission. On the other hand, energy offsets between the Li *K* exciton features in the emission and the excitation spectra provided a measure of the phonon relaxations for these *localized* excitations: the relaxations were found to be 1.0 eV in both materials, similar to the values determined for excitations to the delocalized conduction band states. The energies of the x-ray-emission-based valence band maxima following excitation of the Li *K* exciton are influenced not only by this phonon relaxation but also by the necessity to promote the initially-excited electron into another level when the valence electron recombines with the hole. The measured promotion energies are compared to the experimentally determined core-exciton binding energies.

I. INTRODUCTION

A recent application of soft-x-ray emission (SXE) spectroscopy has been the study of phonon relaxation in insulators.¹⁻⁴ Phonon relaxation refers to the rearrangement of the host lattice ions following formation of a core hole, with the energy liberated by this rearrangement being removed by phonons. This phonon relaxation was first measured in Li (Ref. 5) and Na (Ref. 6) metals by carefully comparing the energy positions of the Fermi edge in SXE and soft-x-ray absorption (SXA) spectra recorded with the same spectrometer. The measured offset is referred to as the Stokes shift; it equals the energy removed by phonons as the ions first rearrange to their new configuration around a core hole and then return to their original positions following annihilation of this hole. The full relaxation energy is quantified as $2\Sigma_{\text{ph}}$,^{1,7} where Σ_{ph} is a measure of the strength of the lattice coupling to the core hole and is referred to as the phonon relaxation energy or phonon self-energy. The measured Stokes shift will equal this full $2\Sigma_{\text{ph}}$ if relaxation of the lattice is complete before the hole is annihilated, whereas in the case of partial relaxation, the measured Stokes shift falls short of $2\Sigma_{\text{ph}}$. The degree of relaxation depends on the balance between the hole lifetime τ and the phonon relaxation time $2\pi/\omega_0$. The phonon relaxation rate is argued to be well characterized by the frequency of the fastest coupled phonon mode in the material. The relaxation rate may be slowed down by bottlenecks, in which case this frequency

represents an upper limit on the rate. For various metals, beginning with Li and Na, the measured shifts are well described by theoretical calculations.^{5,6,8,9}

For semiconductors and insulators one might in principle attempt an analogous measurement of the Stokes shift in which the energy of the conduction-band minimum (CBM) as measured with SXA is compared to the energy of the valence-band maximum (VBM) as measured with SXE. The offset of the VBM below the CBM could then be compared to the band gap of the material, and any additional separation between the measured levels would be attributed to phonon relaxation. In practice the core-level absorption spectra frequently have excitonic structure at the threshold which obscure the onset of absorption to continuum states, and thus the CBM cannot be reliably extracted from these SXA measurements. Another difficulty with this approach is that band gaps are not straightforward to determine from optical absorption data, due largely to valence excitonic features.

An alternative means of measuring the Stokes shift in insulators was recently applied by O'Brien *et al.*¹ to the cation $L_{2,3}$ edges for several oxide insulators: Al₂O₃, MgO, and SiO₂. The binding energies of the relevant core levels (in that instance, $2p$) were determined relative to the valence-band maxima from photoemission spectra, and these binding energies were then compared to the energies of the band maxima as measured in valence SXE spectra. The final states in core-level and valence-band photoelectron emission represent, respectively, the initial

and final states of the x-ray emission process, but in the absence of the lattice relaxation that precedes x-ray emission. As a consequence the difference between the VBM energy in SXE and the photoemission binding energy provides a measurement of the Stokes shift. Substantial shifts, on the order of a volt, were measured in Al_2O_3 , MgO , and SiO_2 . The Stokes shifts of these oxides are much larger than the shifts in Al, Mg, and Si for three reasons: the cation excitations in the ionic insulators are characterized by (1) a larger phonon coupling strength Σ_{ph} , (2) a faster phonon relaxation rate ω_0 , and (3) a longer hole lifetime τ .

The alkali halides represent a class of materials in which the measurement of phonon relaxation is of fundamental interest. Being prototypical ionic compounds, these materials are anticipated to exhibit strong relaxation effects for the same reasons just described in regard to the oxides. The SXA profiles of the alkali halides have been measured and discussed in detail,^{10–12} and these absorption spectra are characterized by a wealth of excitonic features. As mentioned above, such excitonic structure at threshold precludes the extraction of the Stokes shift by comparing the SXA to the SXE spectra. Nevertheless, these excitonic phenomena turn out to yield additional information about phonon coupling in the alkali halides. Excitons screen the hole from the lattice ions, thus altering the phonon-coupling strength Σ_{ph} , and additionally the excitons may influence the lifetime of the core hole τ . Indeed such effects have been measured for B *K* excitations in the insulators B_2O_3 and hexagonal-BN.² In Ref. 2, monochromatic-photon excitation was employed to selectively excite the core-exciton state in these materials. The valence-band SXE spectra in the presence of the exciton were measured and compared to the spectra produced for the higher excitation energies at which no exciton is generated. *K* excitations are advantageous in such studies: spin-orbit splitting in the core level of interest necessitates deconvolution of the spin-orbit contributions when analyzing the absorption or the emission spectra. Finally, it should also be mentioned that in materials with strong excitonic features in absorption, such as the alkali halides, SXE due to direct recombination of these localized excitations can be detected. As described below the energy positions of these excitonic emission features can be compared to the positions of the corresponding excitonic absorption features, thus providing a measure of the phonon relaxation around the exciton.

Li 1s presents a cation *K* level in the range of our spectrometer¹³ and beamline monochromator,¹⁴ and hence Li halides were chosen for the present study. The Li *K* valence emission was observed to decrease in intensity with increasing sample ionicity:¹⁵ LiBr offered the most intense emission, while LiCl was somewhat weaker, and LiF was not readily measurable with monochromatic-light excitation. As will be detailed below, the Li *K* valence emission from all of these Li halides was surprisingly weak when excited with monochromatic light. On the other hand, previous measurements of these materials using electron-beam^{16,17} or white-light^{18,19} excitation have suffered from sample decomposition²⁰ problems.

The most successful of these previous studies is the electron-beam-excited measurement of Arakawa and Williams:¹⁷ for each emitted photon energy these authors recorded the emission as a function of exposure time to the electron beam and then extrapolated the emission intensity to zero time in order to eliminate the influence of the beam.

The present measurements using monochromatic-light excitation suffered from low count rates but were feasible for LiBr and LiCl when performed with our high-efficiency spectrometer,¹³ which employs a two-dimensional multichannel detector. We found that data could be collected without appearance of any metallic Li emission. Photoemission experiments^{21–25} have also been performed successfully on these materials when using monochromatic-light excitation. On the other hand, our electron-beam-excited emission spectra were dominated by the metallic signal even for the shortest exposure times. In addition to reduction of the sample decomposition problem, tunable monochromatic-light excitation was also required in this study to selectively excite core excitons for the purpose of investigating their role in phonon-coupling effects.

II. EXPERIMENTAL

The measurements were performed at Beamline U10A of the National Synchrotron Light Source.¹⁴ The fluorescence spectrometer consists of a toroidal grating and a two-dimensional array detector that is scanned along the Rowland circle defined by the entrance slit and grating.¹³ The entrance slit was fixed at 125 μm , yielding a resolution of 0.16 eV, while the resolution of the beamline monochromator was measured to be 0.2 eV at 60 eV excitation energy and 0.25 eV at 70 eV excitation energy. The energy and bandwidths of the excitation light were directly determined from the light scattered elastically by the sample into the spectrometer. Thus the excitation energy was measured with the same calibration as the x-ray emission. Additionally, the Li *K* excitation spectra were recorded on this same energy scale by measuring the white-light reflection from the samples,²⁶ again using the fluorescence spectrometer. At near-normal incidence (15 degrees off-normal was employed in the present measurements) the reflection varies as $[(n-1)^2+k^2]/[(n+1)^2+k^2]$, where $n+ik$ is the complex index of refraction. For soft x-rays we may usually assume $(n+1)^2 \gg k^2 \gg (n-1)^2$; then the reflectivity follows k^2 and is proportional to the square of the absorption.²⁶ Such measurements have been reported previously for samples of LiF.^{18,19}

The emission and reflectivity spectra are plotted in this paper as photon counts per unit energy interval, and no quantitative compensation for self-absorption has been attempted with the emission spectra. Because of the substantial band gaps in LiBr and LiCl, 7.6 and 9.4 eV,¹¹ respectively, self-absorption should not strongly influence the valence spectra. As will be shown in Sec. III, the exciton emission is partially offset in energy below the exciton feature in absorption, but some self-absorption effects

may influence the upper-energy part of the exciton emission features.

The samples of LiBr and LiCl were bulk crystalline aggregates about 1 cm in diameter. After extended exposure to the beam, these samples showed visible signs of decomposition, but only after prolonged exposure times or excitation with the electron beam could Li *K* emission from Li metal be observed. Nevertheless, the excitation point on the sample was frequently changed.

III. RESULTS AND DISCUSSION

A. Line shapes of the soft-x-ray emission spectra

LiBr emission spectra for excitation photon energies of 72.3 and 79.0 eV are plotted in Fig. 1 as (a) and (b), respectively. The features at roughly 51, 59, and 65 eV are the Li *K* valence emission, the Li *K* exciton emission, and the Br $M_{4,5}$ valence emission, respectively. The Br $M_{4,5}$ emission is not generated by the 72.3 eV excitation energy. The emission spectra in Fig. 1 are in qualitative agreement with the electron-beam-excited spectrum of Arakawa and Williams.¹⁷ The overall resolution of the present photon-excited data is improved: the Li *K* valence, Li *K* exciton, and Br $M_{4,5}$ valence emission features have full widths at half maximum of about 3, 2, and 2.5 eV, whereas the features of Arakawa and Williams are roughly 25% wider.²⁷ For comparison, the width of the LiBr valence band as measured by photoemission is about 3 eV.²³ The enhanced resolution of the present emission measurements will prove useful below when we

will wish to precisely quantify the energy positions of various spectral features.

Valence emission spectra represent the *local partial* density of states (DOS) based on the dipole selection rule governing the radiative transition of a valence electron dropping to fill a core hole. The Li *K* emission from LiBr is based on the weak overlap of the Br-4*p*-derived valence-band states with the Li *K* hole, whereas the Br $M_{4,5}$ emission involves a stronger direct overlap. The valence *photoelectron* emission process is governed by the matrix element between the valence electronic states and the delocalized states of the outgoing photoelectrons, and thus valence photoemission spectra represent a nonlocal DOS. It is of interest to compare the three LiBr valence-band DOS measurements: valence emission spectra for both Li *K* and Br $M_{4,5}$ excitations and a valence photoemission spectrum.

In the valence photoemission spectra of LiBr a double-humped line shape is observed,^{21,23–25} and in Fig. 1, a similar structure is seen in the Li *K* valence emission feature. In Fig. 2, Li *K* valence emission spectra for three different excitation energies are superimposed for comparison on a photoemission spectrum taken from Johansson and Hagström.²⁴ The photoemission spectrum was excited with Mg K_{α} radiation at 1253.6 eV. The SXE spectra have been converted to DOS through division by photon-energy-cubed, and they were then matched to the photoemission spectrum by normalizing the intensities, adding the same background as in the photoemission spectrum,²⁸ and aligning the valence-band maxima. The overall similarity in the DOS as derived from photoemission and Li *K* emission is apparent in Fig. 2, with all spectra exhibiting a main peak at -2 eV binding energy and a more-negative-binding-energy shoulder.

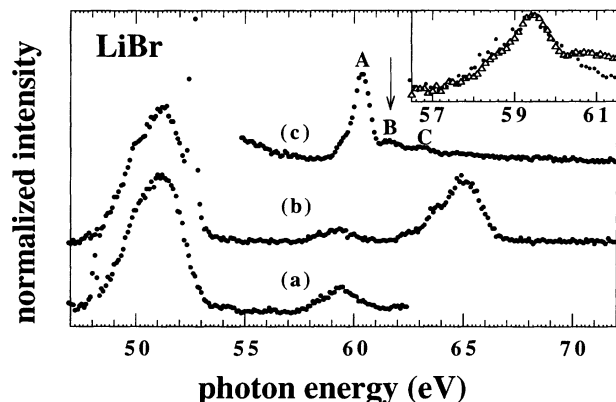


FIG. 1. In (a) and (b), the soft x-ray emission from LiBr is plotted for excitation energies of 72.3 and 79.0 eV, respectively. The two spectra are normalized to equal intensity of the Li *K* valence feature at 51 eV. The sharp peaks observed at 48.2 eV in (a) and 52.7 eV in (b) lie at exactly two-thirds of the excitation energy and are due to second-order light from the beamline monochromator, seen in third order in the spectrometer. In (a), this feature has been reduced using an Al filter in the beamline monochromator to attenuate the second-order excitation, whereas in (b), this strategy was not used because the primary excitation energy was itself above the Al edge. In (c), the white-light reflectivity from the same sample is plotted. In the inset the exciton features extracted from spectrum (a), filled circles, and spectrum (c), open triangles, are compared as described in the text.

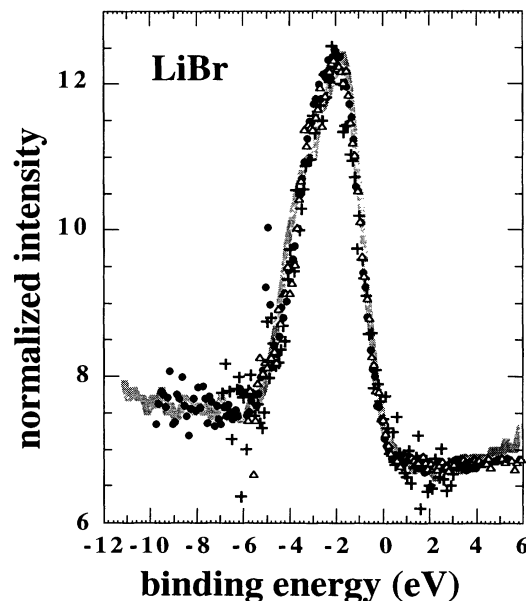


FIG. 2. Li *K* valence emission spectra from LiBr taken with excitation energies at 72.3 eV (closed circles), 67.5 eV (open triangles), and 59.7 eV (crosses) are superimposed on a valence photoemission spectrum from Ref. 24 (solid gray line) as described in the text.

The photoemission spectrum is somewhat wider due to the greater instrumental broadening, 1.3 eV versus the 0.16 eV bandwidth of the spectrometer used in the SXE measurement.

The Br $M_{4,5}$ emission feature in Fig. 1 involves the complication of a 1.05 eV spin-orbit splitting in the core level,²⁹ and deconvolution of the M_4 and M_5 emission components was carried out using a standard procedure.³⁰ This procedure requires the intensity ratio of the M_5 to the M_4 emission component. A ratio of 1.5, the statistical value, was initially tried, but the only sensible decompositions were achieved with nonstatistical ratios in the range of 0.7 (Fig. 3). The basis of this nonstatistical ratio is now considered. As detailed below, the thresholds for excitations of the M_5 and M_4 electrons to the continuum are 74.3 and 75.3 eV, respectively, and as the excitation energy is raised above these thresholds, the M_5 and M_4 absorption decreases rapidly.³¹ For a 79.0 eV excitation energy the M_5 and M_4 electrons are excited 4.7 and 3.7 eV above threshold, respectively; this one volt separation relative to threshold may account for the suppressed intensity of the M_5 emission with respect to the M_4 . On the other hand, this excitation is sufficiently high in the s - p -derived conduction band of LiBr that it should not be influenced by intermediate coupling effects such as are seen to reduce branching ratios in $L_{2,3}$ excitonic absorption features.²⁶ Self-absorption may in general also influence measured branching ratios; however, in the case of LiBr, the absorption does not appear to vary substantially across the energy range of the Br $M_{4,5}$ emission (Fig. 1).

In Fig. 3, the extracted M_5 component of the Br $M_{4,5}$

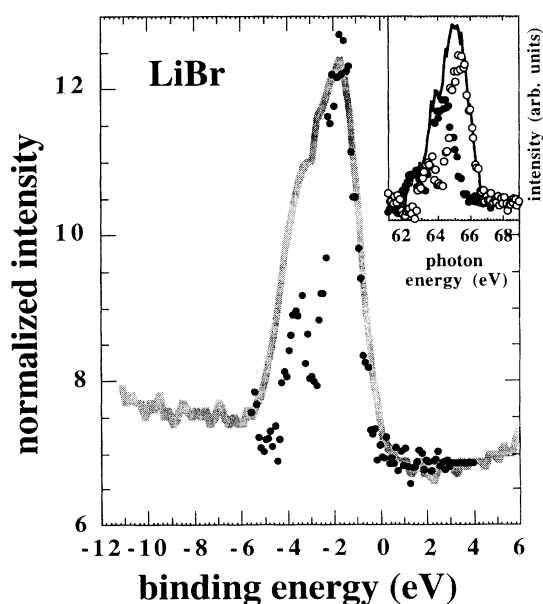


FIG. 3. A Br M_5 valence emission spectrum from LiBr taken with an excitation energy of 79.0 eV is superimposed on a valence photoemission spectrum from Ref. 24 (solid gray line) as described in the text. In the inset the decomposition of the Br $M_{4,5}$ valence emission spectrum into its M_4 (open circles) and M_5 (closed circles) components is shown.

valence emission is shifted to align its VBM with that of the valence photoemission spectrum, analogous to Fig. 2. The Br M_5 x-ray emission spectrum consists of two peaks at the same locations as the peaks in the photoemission and Li K emission spectra, supporting the validity of the procedure used to deconvolute the spin-orbit components. The Br spectrum is also in qualitative agreement with the two-peaked $4p$ valence band calculated by Kunz and Lipari.³² On the other hand, this Br spectrum is substantially narrower than its Li K counterpart. As will be detailed below, the lifetimes of the Br M_5 and Li K excitations are difficult to measure for LiBr, but rough estimates indicate that the Br M_5 lifetime width should be greater than that of Li K. We will also show that the phonon broadenings for these two levels are expected to be similar. The width of emission spectra may also be influenced by self-absorption, but as noted above, self-absorption is not anticipated to substantially distort the line shape of the Br $M_{4,5}$ emission. Thus, the narrowness of the Br M_5 spectrum relative to the other valence spectra is a bit surprising.

The emission spectrum for LiCl taken with an excitation energy of 72.3 eV is plotted in Fig. 4(a). Here the features at roughly 50 and 60 eV are the Li K valence and Li K exciton emission, respectively. In general for this study, the LiCl emission data are noisier than the LiBr data because the emission intensity of the chloride is only about half that of the bromide. The Li K emission from both LiBr and LiCl is weak relative to the B K emission from BN and B₂O₃ even though B is a comparably low-atomic-number element. The particularly low intensity of the Li K SXE in the Li halides may be a consequence of the strong ionicity of these materials: the valence electrons can virtually be treated as Br $4p$ and Cl $3p$ electrons in LiBr and LiCl, respectively. The limited overlap of these valence electrons with the Li $1s$ hole is anticipated to suppress both the radiative and nonradiative decay rates, whereas the low SXE intensities are indicative of a

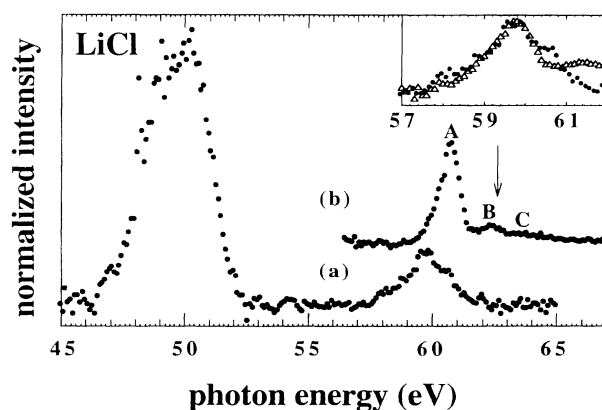


FIG. 4. In (a), the soft x-ray emission from LiCl is plotted for an excitation energy of 72.3 eV. Also, the sharp two-thirds peak lies at 48.2 eV. In (b), the white-light reflectivity from the sample is plotted. In the inset the exciton features extracted from spectrum (a), filled circles, and spectrum (b), open triangles, are compared as described in the text.

low fluorescent *yield*, i.e., a low ratio of the radiative rate relative to the total decay rate. It is difficult without a detailed calculation to estimate the influence of the sample ionicity on the fluorescent yield. However, the fact that the cation *K* valence emission intensity drops in going from LiBr to LiCl to LiF (Ref. 15) as well as in going from the boron to the lithium compounds provides empirical evidence that the fluorescent yield falls with increasing ionicity.

As with LiBr the agreement of the LiCl emission with the electron-excited data of Arakawa and Williams¹⁷ is good. The full widths at half maximum of the valence and exciton emission features are 3 and 2 eV; again the line shapes of the electron-beam-excited features in Ref. 17 are not as well resolved. The width of the valence band as measured with photoemission is about 3 eV.²² In Fig. 5, Li *K* valence emission spectra from LiCl are superimposed on a photoemission spectrum taken from Johansson and Hagström²⁴ in the manner described above for LiBr. Again, the overall similarity between the Li *K* SXE and photoelectron emission spectra is apparent, with a main valence peak and a more-negative-binding-energy shoulder. In both the photoemission and the SXE spectra the shoulder is higher in intensity for LiCl than for LiBr.

B. Excitation spectra from white-light reflectivity

The white-light reflectivities for LiBr and LiCl are plotted as Figs. 1(c) and 4(b), respectively. The features of these excitation spectra lie at nearly the same energies as the features in the transmission absorption measurements of Haensel, Kunz, and Sonntag (see Table I).¹⁰ Common to the reflectivity and transmission measure-

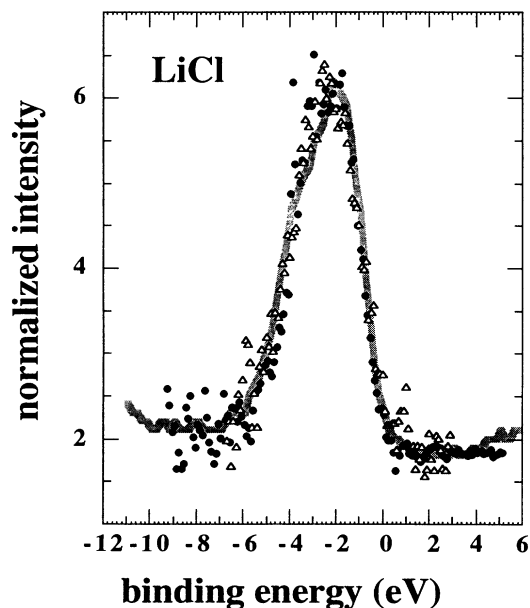


FIG. 5. Li *K* valence emission spectra from LiCl taken with excitation energies of 72.3 eV (closed circles) and 60.4 eV (open triangles) are superimposed on a valence photoemission spectrum from Ref. 24 (solid gray line) as described in the text.

TABLE I. Near-threshold peak positions in the reflectivity and transmission measurements of Li *K* excitation spectra. All energies are given in eV.

Sample	Feature	Reflectivity	Transmission (Ref. 10)
LiBr	A	60.4±0.07	60.44±0.07
	B	61.7±0.2	61.68±0.07
	C	63.2±0.2	62.96±0.07
LiCl	A	60.75±0.07	60.75±0.07
	B	62.4±0.2	62.27±0.07
	C	63.7±0.2	63.54±0.07

ments of both LiBr and LiCl is a dominant excitonic peak at the absorption threshold. Adopting the labeling of Haensel, Kunz, and Sonntag, this main exciton feature is designated A, and two weaker, higher-energy features are designated B and C. Peak A in the Li *K* excitation spectra as measured by either reflectivity or transmission exhibits a distinct low-energy shoulder, and as seen in Figs. 1 and 4, an analogous shoulder appears on the low-energy side of the *emission* excitonic features. However, the emission features are located at lower energies than the respective excitation features. In the insets to these figures, the excitonic features are compared by shifting the excitation peaks onto their emission counterparts. The shifts demonstrate a good match in line shape, including the main peak and its low-energy shoulder. In these insets the emission spectra have been divided by photon-energy-cubed, while the reflectivities have been converted to absorption by subtracting the background and taking the square root.

Pantelides¹¹ established the position of the CBM in the absorption spectra of various alkali halides by taking the binding energy of the relevant core level with respect to the VBM as measured by photoemission and adding the band gap as measured by optical absorption. Johansson and Hagström²⁴ have since measured Li *1s* binding energies in LiBr and LiCl, specifically to calibrate core excitations, and they have determined these energies to be 54.1 and 53.2 eV, respectively. Adding the LiBr and LiCl band gaps of 7.6 and 9.4 eV,^{11,33} we arrive at 61.7 and 62.6 eV for the location of the CBM with respect to the Li *1s* core levels. These thresholds for excitation to the continuum are marked by arrows on Figs. 1 and 4. So, based on the *1s* binding energies of Johansson and Hagström together with the peak-A-energy positions in our absorption spectra (or equivalently those of Haensel, Kunz, and Sonntag), the Li *K* exciton binding energies are determined to be 1.3 and 1.85 eV for LiBr and LiCl, respectively. An independent measurement of these binding energies cannot necessarily be derived from the Li *K* valence and Li *K* exciton *emission* features in Figs. 1 and 4 because, as explained below, the exciton and valence emission features can exhibit different phonon relaxation shifts. The various excitation thresholds and binding energies for LiBr and LiCl are summarized in Table II. Note that the error range for the entries in rows 1, 3, 5, and 6 of this table exceeds plus-or-minus 0.3 eV. These

TABLE II. Excitation thresholds and binding energies for LiBr and LiCl. All energies are given in eV.

Threshold or binding energy		Source	LiBr	LiCl
R1	Band gap	Optical absorption ^a	7.6±0.3	9.4±0.3
R2	Li <i>K</i> binding energy relative to VBM	Photoemission ^b	54.1±0.1	53.2±0.1
R3	Threshold for Li <i>K</i> excitations to CBM	R1+R2	61.7±0.4	62.6±0.4
R4	Main Li <i>K</i> exciton creation energy	Reflectivity, Table I	60.4±0.07	60.75±0.07
R5	Exciton binding energy relative to CBM	R3-R4	1.3±0.47	1.85±0.47
R6	Threshold for Li <i>K</i> exciton creation via shakeup	R1+R4	68.0±0.37	70.15±0.37

^aReferences 11 and 33.

^bReference 24.

errors derive primarily from the uncertainty in the band gap.³⁴

Now that the excitation spectra have been presented, we observe that the Li *K* exciton feature is present in the emission spectra of Figs. 1 and 4 despite the fact that the excitation energy is not set at the value for direct exciton creation. The absorption measurements have established the main exciton-creation energies to be 60.4 and 60.75 eV in LiBr and LiCl, respectively. The emission from the exciton cannot be measured when the excitation energy is set at this creation energy because the emission then coincides in energy with the substantially more intense elastically scattered excitation radiation which is also measured in the spectrometer. This problem complicated earlier efforts to measure Li *K* exciton emission in LiF using white-light excitation.^{18,19} However, O'Brien *et al.*² have demonstrated that when the monochromatized excitation-phonon energy exceeds the exciton-creation energy by an amount equal to or greater than the band gap, the exciton can once more be populated through multielectron shakeup processes; then its decay through radiative emission may be observed. For LiBr this threshold for exciton population through shakeup is 68.0 eV (60.4 eV plus the band-gap energy of 7.6 eV), while for LiCl this threshold is 70.15 eV. The excitation energies used to generate the emission spectra of Figs. 1 and 4 exceed these thresholds. In Fig. 6, the onset of the exciton emission in LiBr as the exciton energy is increased through the 68.0 eV shakeup threshold is illustrated. It is not presently understood why the exciton emission intensity is diminished for the 79.0 eV excitation energy.

C. Nature of the shoulder on the main exciton

We consider now the low-energy shoulder observed on the Li *K* exciton features in the emission and excitation spectra (Figs. 1, 4, and 6). The shoulder is also clearly present in the Li *K* SXA data of Haensel, Kunz, and Sonntag¹⁰ which include the LiF spectrum. In both the emission and excitation spectra the shoulder is separated from the main exciton peak by about 1 eV.

Ichikawa *et al.*⁵ also observed a low-energy exciton shoulder in their Auger yield and constant-initial-state (CIS) measurements of Li *K* absorption in LiBr and LiCl. Variations in the LiCl shoulder intensity as a function of incident-light angle led these authors to conclude that the lower-energy peak in their surface-sensitive measurements is a surface exciton.³⁵ However, the transmission

absorption measurements of Haensel, Kunz, and Sonntag¹⁰ and the present reflectivity and emission experiments are manifestly bulk sensitive. Ichikawa *et al.* may very well have observed a surface exciton, but this must be distinct from the shoulder of interest here: indeed the low-energy shoulder in the CIS spectra of Ref. 35 has a separation from the main peak that exceeds 1 eV, and its strong intensity is likely obscuring the bulk-derived shoulder.

A low-energy component has also been observed in the B *K* exciton emission of B₂O₃ (Refs. 2 and 4) and BN (Refs. 2, 36, and 37), but in these materials a corresponding component does not appear in the absorption spectra.^{4,38} The shoulder on the B *K* exciton emission features was interpreted in terms of phonon ringing,⁴ motivated by the absence of the shoulder in SXA and the

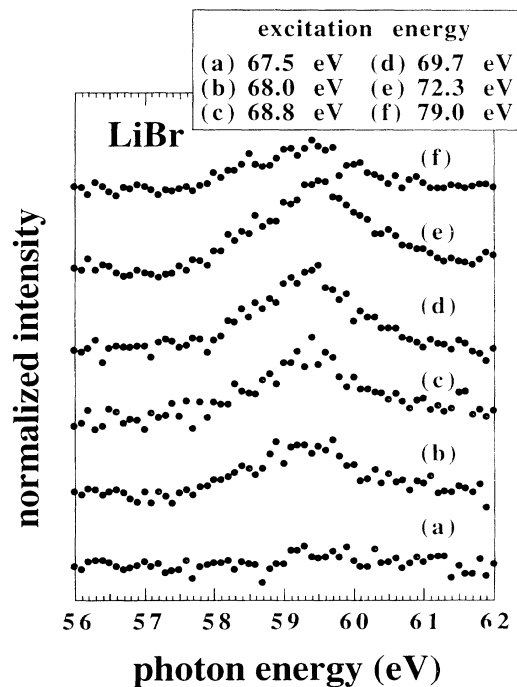


FIG. 6. The Li *K*-exciton soft x-ray emission from LiBr is plotted as the excitation energy is varied through the threshold for exciton population via a shakeup process, 68.0 eV. The six spectra are normalized to equal intensity of the Li *K* valence feature, which lies below the energy range of this figure at 51 eV.

large (2 eV) component separation in SXE.³⁹ In the case of the present Li *K* data, the shoulder does appear in the absorption spectra, and in addition the smaller 1 eV separation of the Li *K* exciton components suggests that the phonon ringing interpretation does not apply to the Li compounds.

The exciton shoulder most plausibly corresponds to the lowest-lying *s*-symmetry exciton, which in an atom is dipole-forbidden for *K* excitations. Fields, Gibbons, and Schnatterly⁴⁰ have recorded the Li *K* absorption spectrum of LiF using inelastic electron scattering. With this technique the same dipole selection rule applies at low transferred momentum *q*, but at higher *q* these rules break down. Observing that the shoulder peak is enhanced at high *q*, the authors argue that this peak is indeed the dipole-forbidden exciton. Zunger and Freeman⁴¹ have calculated in the local-density formalism the ground-state energy levels of LiF as well as its Li *K* excitations. Their results support the identification of the main exciton and its shoulder in the excitation spectrum as the lowest-lying *p* and *s* excitons. Furthermore, they point out the similarity of the SXA exciton energies to the excitation energies of the isolated Li¹⁺ ion: 60.8 and 62.2 eV for the transitions to $2s\ ^1S_0$ and $2p\ ^1P_0$ states, respectively.⁴² Fields, Gibbons, and Schnatterly⁴⁰ have suggested that the strength of the forbidden transition in the absorption spectra is another manifestation of phonons, which break the symmetry underpinning the dipole selection rules.

The onset of the Li *K* exciton emission feature in LiBr following shakeup excitation, shown in Fig. 6, must now be considered. It appears that the exciton emission shoulder may turn on simultaneously with the onset of the main peak, in apparent contrast to B *K* emission.^{2,39} For multielectron excitations the dipole selection rules are applied to the quantum numbers of the full initial and final states, and the excitation of the *s*-symmetry exciton is no longer necessarily forbidden. However, the shoulder in emission is still weaker than the main line intensity because the *emission* transition is still dipole-forbidden. If indeed the shoulder peak does not turn on by itself at 1 eV lower excitation energy than the main peak (the onset of the shoulder had been anticipated at roughly 67.0 eV excitation energy), this observation demands further interpretation. The primary excitation of the *s*-exciton may occur via initial *p*-exciton creation followed by a fast *p*-to-*s* exciton transition radiating in the infrared. Such a transition has been suggested by Jackson and Pederson⁴³ in the context of the C *K* exciton of diamond. Quantitative theoretical evaluation of the *s* and *p* exciton picture with respect to the results of Figs. 1, 4, and 6 is beyond the scope of this present study.

D. Energy positions and Stokes shifts of emission spectra

For LiBr the match between the emission and absorption exciton features (Fig. 1, inset) was achieved by shifting the absorption profile 1.0 eV to lower energy, while the match for LiCl (Fig. 4, inset) was also achieved by a 1.0 eV shift. For these two Li halides this 1.0 eV shift is the Stokes shift for the main localized Li *K* excitation.

Arakawa and Williams¹⁷ in their electron-beam-excitation study, first pointed out the energy offset between their SXE excitonic features and the SXA excitons measured by Haensel, Kunz, and Sonntag.¹⁰ In the present paper the offset can be precisely quantified for two reasons. First, the exciton line shape that had been observed in the absorption is now resolved in the emission as well. Second, the absorption and emission measurements presented in Figs. 1 and 4 were made consecutively on the same spectrometer to avoid relative calibration errors. These 1.0 eV Stokes shifts reflect the phonon relaxation that takes place between creation of the exciton and its subsequent recombination. Analogs to peaks *B* and *C* in the LiBr and LiCl absorption are not observed in the emission spectra. These peaks, like the main peak *A*, have been attributed by Pantelides¹¹ to excitonic phenomena. Localized excited states associated with these peaks may decay to the lowest-energy exciton state before recombining; another possibility is rapid autoionization to continuum states.

Figures 7 and 8 show the dependence of the Li *K* valence emission on excitation-photon energy for LiBr and LiCl, respectively. The LiCl data exhibit poorer statistics than the best LiBr data, largely because of the lower emission intensity from the LiCl. The emission spectra in these figures are normalized to equal intensity in order to facilitate comparisons of line shape and energy position. The measured intensities exhibited a gradual systematic rise as a function of excitation energy and showed no discontinuous jump as the excitation energy was raised from the exciton-creation values at threshold

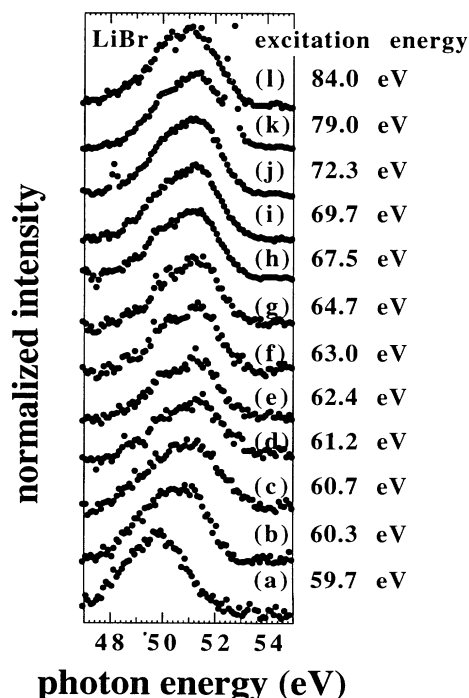


FIG. 7. Li *K* valence soft x-ray emission spectra from LiBr are plotted for various excitation energies. The 12 spectra are normalized to equal intensity.

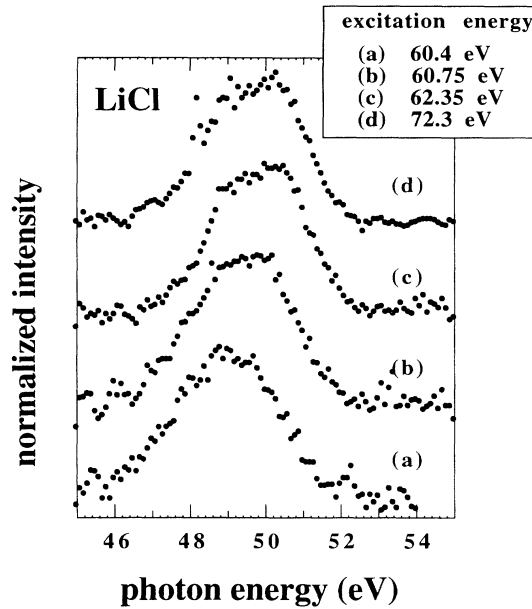


FIG. 8. Li *K* valence soft x-ray emission spectra from LiCl are plotted for various excitation energies. The four spectra are normalized to equal intensity.

to conduction-band-transition values. The Li *K* valence emission for excitation energies set at exciton-creation values will be termed *spectator* emission. On the other hand, when the excitation energy is raised above these creation energies, the valence emission occurs without an exciton, and this process will be referred to as *normal* emission. As mentioned above, when the photon energy is raised above an exciton-creation energy by more than the band gap, the exciton can again be populated through shakeup processes. For excitation energies above this second threshold, the valence emission will consist of a combination of spectator and normal emission.

For Li *K* emission from LiBr, the range of excitation energies yielding normal emission extends from 61.7 to 68.0 eV (Table II) and is thus represented by spectra (e) through (h) in Fig. 7. The absorption features *B* and *C* lie at the beginning of this range (at 61.7 and 63.2 eV, respectively), but Pantelides¹¹ has attributed these features to excitonic phenomena because of their strong intensity relative to the calculated conduction-band DOS. The valence band spectra (e) through (h) are essentially identical in line shape and energy position. The Stokes shift of these normal emission spectra can be determined in the manner described in Sec. I: by comparing the position of

the valence-band maxima in these spectra to the Li *1s* binding energy as determined from photoemission. As mentioned in Sec. III B, Mg *K_α*-excited valence and core-level photoemission spectra were measured by Johansson and Hagström²⁴ for this purpose of calibrating core excitations. The extraction of the VBM from either SXE or photoemission spectra typically involves fitting the data near the top of the band with some DOS function convolved with instrumental and lifetime broadening. To avoid a discrepancy between our method of SXE-VBM extraction and the method used by Johansson and Hagström for photoemission-VBM extraction, we established the VBM of the SXE spectra by directly aligning these spectra to the photoemission spectrum (reproduced in Fig. 2), paying particular attention to the alignment at the maxima.⁴⁴ The valence-band maxima of the normal Li *K* valence emission spectra from LiBr were determined in this manner to lie at 53.1 eV. On the other hand, the binding energy of the Li *1s* core level as measured with photoemission is 54.1 eV. The difference between these two values, 1.0 eV, represents the Stokes shift of the normal Li *K* valence emission in LiBr.

Spectra (a) through (d) in Fig. 7 represent spectator emission: the excitation energies for (a), (b), and (c) lie on the main exciton peak *A* of the absorption profile, while that for (d) lies on the smaller peak *B*. A measurement of the valence emission for an excitation energy on the SXA excitonic-shoulder component at 59.3 eV was also attempted, but the emission intensity was insufficient to yield a result. The spectator Li *K* valence emission spectra corresponding to excitations on peak *A* exhibit a shift to lower energy, while spectrum (d) is unshifted with respect to the normal spectra. Spectrum (a), taken with the excitation energy toward the low-energy edge of peak *A*, exhibits the greatest shift, about 1.2 eV, but in line shape it closely resembles the normal valence emission spectra, as shown in Fig. 2. Spectra (b) and (c) exhibit an intermediate shift and are additionally somewhat broadened relative to spectra (a) and (e) through (h). Apparently (b) and (c) constitute a mix of spectator and normal emission in which the center of the excitation band yields spectator emission while the high-energy tail of the exciting radiation still produces significant normal emission. We will consider spectrum (a) to represent a relatively pure spectator emission spectrum. Aligning it with the photoemission valence band spectrum, a VBM energy of 51.9 eV is determined, and the total shift for the spectator emission spectrum is thus established to be 2.2 eV. Both the normal and spectator shifts of LiBr are entered in Table III.

TABLE III. Li *K* spectral shifts between excitation and emission. All energies are given in eV.

	Spectral feature	Source	LiBr shift	LiCl shift
R1	Exciton	SXE and reflectivity	1.0±0.05	1.0±0.05
R2	Normal valence	SXE and photoemission	1.0±0.15	1.2±0.15
R3	Spectator valence	SXE and photoemission	2.2±0.15	1.9±0.15
R3a	Spectator: phonon relaxation	R1	1.0±0.05	1.0±0.05
R3b	Spectator: promotion	R3-R1	1.2±0.20	0.9±0.20

As mentioned above, spectra (d), (e), and (f) were generated with excitation energies in the range of peaks *B* and *C* of the absorption profile. Pantelides¹¹ suggested that these are excitonic in origin, but it was noted above that unlike peak *A*, no features appear in the emission spectra that can be attributed to direct recombination of localized excited states *B* and *C*. At first it was suggested that these higher-energy localized states might decay rapidly to the primary exciton associated with *A*. However, we now observe that the Li *K* valence spectra generated by excitations *B* and *C* are indistinguishable from normal emission spectra. If peaks *B* and *C* do indeed represent localized excited states, as suggested by Pantelides, these states must rapidly autoionize to continuum states.

Spectra in Fig. 7 taken with excitation energies exceeding the threshold for shakeup exciton creation, 68.0 eV, are anticipated to consist of both spectator and normal emission. In fact, however, spectra (i) through (l) are very similar in line shape and position to the purely normal emission spectra of (e) through (h). Figure 2 demonstrates the similarity between spectra (h) and (j), both of which were shifted a total of 53.1 eV to appear on the binding energy scale of the figure. From the dominance of the normal-emission contribution to the spectra in the shakeup regime, (i) through (l), we conclude that the shakeup excitations of the core exciton are not very probable; those excitations that do occur must decay largely by direct recombination to yield the exciton emission features seen in Figs. 1 and 6.

For LiCl the range of excitations corresponding to normal excitation is 62.6 through 70.15 eV, and none of the data in Fig. 8 were taken in this range. However, the fact that the emission spectra recorded with excitation energies of 62.35 and 72.3 eV have essentially identical spectral line shapes and positions suggests that, analogous to the LiBr data, the spectra (c) and (d) accurately represent normal valence emission. The valence-band maxima of these spectra are determined by aligning them with the LiCl valence photoemission spectrum of Johansson and Hagström, as shown in Fig. 5, and these maxima are established to lie at 52.0 eV. Since the photoemission-based Li 1s binding energy in LiCl is reported by these authors as 53.2 eV, the Stokes shift of the normal emission is 1.2 eV. The spectator emission spectra (a) and (b) are shifted to lower photon energy with respect to the normal spectra, and again spectrum (a), with its excitation energy toward the low-energy edge of the main exciton peak, is taken to represent a relatively pure spectator emission spectrum. Its valence-band maximum is determined to lie at 51.3 eV, thereby yielding a spectator shift for LiCl of 1.9 eV.

The binding energy of the Br 3*d* core level is given by Johansson and Hagström without discriminating the two spin-orbit components. Their Br 3*d* core level spectrum is plotted in this reference, and we reanalyzed it with a spin-orbit splitting of 1.05 (Ref. 29) and a statistical branching ratio of 1.5, yielding a Br 3*d*_{5/2} binding energy of 66.7 eV. Adding the LiBr band-gap energy of 7.6 eV, it is concluded that the threshold for transitions from the Br 3*d*_{5/2} level to the conduction band is 74.3 eV. An excitation energy of 79.0 eV promotes Br 3*d*_{5/2} electrons to

4.7 eV above the CBM, and this excitation gives rise to a normal Br *M*₅ valence emission spectrum. In Fig. 3, this emission spectrum was shifted by 66.0 eV to align its VBM with that of the valence photoemission spectrum of Johansson and Hagström; 66.0 eV is thus the position of the VBM in the Br *M*₅ emission spectrum. Comparing this 66.0 eV value to the Br 3*d*_{5/2} binding energy, 66.7 eV, a Stokes shift of 0.7 eV is established for normal Br *M*_{4,5} excitations.

E. Interpretations of spectral shifts: phonon relaxation and promotion energies

The Stokes shifts for normal Li *K* excitations were found to be 1.0 and 1.2 eV in LiBr and LiCl, respectively. These shifts characterize the phonon relaxation and emission processes, and they can be evaluated in the context of parameters that determine the phonon coupling, specifically, the phonon relaxation energy Σ_{ph} , the hole lifetime τ , and the phonon relaxation rate ω_0 . Citrin, Eisenberger, and Hamann⁴⁵ demonstrated that phonon coupling also influences the width of core-level photoemission spectra, and they related this phonon broadening to the phonon-coupling parameters. These authors assert that the longitudinal optical (LO) phonon mode dominates the phonon-coupling process in the ionic alkali halides, and since this mode generally exhibits little dispersion, a single-frequency Einstein model of the phonons was used to evaluate this coupling. Then the following formula for the standard deviation σ_{ph} of the phonon broadening can be employed:

$$\sigma_{\text{ph}}^2 = \hbar\omega_{\text{LO}}\Sigma_{\text{ph}} \coth(\hbar\omega_{\text{LO}}/2kT), \quad (1)$$

where ω_{LO} is the frequency of the LO mode. These authors furthermore used the following formula for Σ_{ph} , derived from an electron-phonon interaction Hamiltonian:

$$\Sigma_{\text{ph}} = e^2(6/\pi V_m)^{1/3}(1/\epsilon_\infty - 1/\epsilon_0), \quad (2)$$

where V_m is the volume of the primitive unit cell, and ϵ_∞ and ϵ_0 are their high-frequency and low-frequency dielectric constants. Based on formulas (1) and (2), Citrin, Eisenberger, and Hamann calculated phonon broadenings that accurately reproduce the temperature dependence of K 2*p* core-level widths from KF, KCl, and KI, although the absolute magnitudes of the calculated σ_{ph} were systematically smaller than the measurements. Mahan⁴⁶ later recalculated Σ_{ph} and σ_{ph} for various alkali halides based on summations over all phonon modes, and his σ_{ph} agree closely with the measurements of Citrin, Eisenberger, and Hamann. Mahan observed that the values of Σ_{ph} based on formula (2) are generally too small by a factor of 2.

In Table IV, values of Σ_{ph} based on formula (2) are listed for LiF, LiCl, and LiBr. Mahan could perform his more sophisticated computations of Σ_{ph} and σ_{ph} only for alkali halides which had had their phonon dispersion characterized, for example by neutron scattering. While the phonon dispersion of LiF has been measured by Dol-

TABLE IV. Parameters related to phonon broadening and relaxation in the Li halides.

Sample	Cation-anion distance (Å)	ϵ_∞	ϵ_0	Σ_{ph} (eV) formula (2)	Σ_{ph} (eV), scaled by 1.7	$\hbar\omega_0$ (eV), $\hbar\omega_{\text{LO}}$ at X
LiF	2.014 ^a	1.92 ^b	9.01 ^c	2.89	4.99 ^e	0.057 ^f
LiCl	2.570 ^a	2.75 ^b	11.95 ^d	1.54	2.7	0.029 ^g
LiBr	2.751 ^a	3.16 ^b	13.25 ^d	1.24	2.15	0.023 ^g

^aExperimental, Ref. 47.

^bExperimental, Ref. 48.

^cExperimental, Ref. 49.

^dExperimental, Ref. 50.

^eTheoretical, Ref. 46.

^fExperimental, Ref. 51.

^gTheoretical, Ref. 52.

ling *et al.*⁵¹ no such studies of LiBr and LiCl appear to be available, even up to the present time. Mahan's results for Σ_{ph} are slightly different for cation and anion holes, unlike values based on formula (2), and his Σ_{ph} for Li holes in LiF, 4.99 eV, is entered in Table IV. This is larger than the 2.89 eV derived from formula (2) by 1.7 times, nearly the factor of 2 specified by Mahan. In Table IV, adjusted estimated of Σ_{ph} for LiBr and LiCl are given, scaled by this multiplicative factor of 1.7. Then $2\Sigma_{\text{ph}}$ is approximated to be 4.3 and 5.4 eV in LiBr and LiCl, respectively, and these values can be compared to the measured phonon relaxations for normal Li *K* excitations in these two materials, 1.0 and 1.2 eV. This suggests that partial relaxation takes place in these ionic materials, similar to the finding for the oxide insulators.¹

Partial relaxation occurs when the hole lifetime τ and the phonon relaxation time $2\pi/\omega_0$ are roughly equal. For the alkali halides the fastest coupled mode is again the LO mode appearing in formula (1), and hence ω_{LO} is the relevant estimate of ω_0 . Mahan⁴⁶ has observed that the frequency ω_{LO} at the *X* point in the Brillouin zone accurately represents the average of this rather nondispersive mode over the zone. In Table IV, $\hbar\omega_{\text{LO}}(X)$ is listed for the three Li halides. The value for LiF is taken from the neutron scattering study of Dolling *et al.*,⁵¹ while the values for LiBr and LiCl are based on calculations by Sanjeeviraja *et al.*,⁵² whose theoretical results exhibit good agreement with all of the *measured* alkali-halide dispersions. It remains to compare the phonon relaxation times to the hole lifetimes or equivalently to compare the phonon energies $\hbar\omega_{\text{LO}}$ in Table IV to the lifetime widths Γ (equal to h/τ) for Li *K* excitations. Unfortunately, the Li *1s* lifetimes in the Li halides are difficult to measure. As Citrin, Eisenberger, and Hamann⁴⁵ point out, the strong phonon broadening of photoemission core levels in these ionic materials precludes an accurate extraction of the lifetime width. However, Γ has been extracted precisely for the Li *1s* core level in Li metal, which has a smaller phonon broadening.⁵³ This lifetime width of 0.04 eV is not directly applicable to Li halides: the valence electron density around the Li atom is substantially reduced in the ionic compounds, thus increasing the lifetime and reducing Γ . We can only conclude that for Li *K* excitations in the Li halides, Γ is less than 0.04 eV. Considering the values of $\hbar\omega_0$ in Table IV, nor-

mal Li *K* excitations in the Li halides are expected either partial or complete relaxation. Our above measurements indicate that partial relaxation takes place in LiBr and LiCl.

The phonon relaxation shift for the normal Br $M_{4,5}$ excitation in LiBr is 0.7 eV, 0.3 eV less than the shift for the normal Li *K* excitation. To first order the phonon relaxation energy Σ_{ph} is the same for the Li *K* and Br $M_{4,5}$ excitations in LiBr. This is the prediction of formula (2) and is roughly supported by the more detailed calculations of Mahan.⁴⁶ The phonon relaxation rate ω_0 is also anticipated to be nearly the same for the two excitations since in either case LO modes are anticipated to dominate. However, the hole lifetime will depend on both the specific elemental level in which the hole is created and, as mentioned above, chemical effects in the valence electron density around the hole. The lifetime width Γ for $M_{4,5}$ excitations in atomic Br is interpolated from the calculations of McGuire⁵⁴ to be 0.08 eV. For Br in LiBr, the valence electron density is enhanced relative to the atomic state, and thus, opposite to Li, the lifetime width Γ should increase. Hence, it makes sense that the phonon relaxation for normal Br $M_{4,5}$ excitations in LiBr is less complete than for normal Li *K* excitations.

The shifts of the spectator Li *K* valence emission are 2.2 and 1.9 eV in LiBr and LiCl, respectively. However, unlike Stokes shifts in the normal valence emission spectra, these values represent more than just the phonon relaxation between exciton creation and spectator valence emission. Indeed the relaxation shift itself should be the same as that measured from the exciton emission and absorption features because the same phonon-coupling strength Σ_{ph} , hole lifetime τ , and phonon relaxation rate ω_0 apply, independent of the final decay process of the exciton. However, there is an additional source of shift in the spectator valence emission spectra, which O'Brien *et al.*² first pointed out in B *K* emission from B_2O_3 and BN. When the spectator valence emission transition annihilates the core hole, the electron in the exciton state, i.e., the initially-excited electron, can no longer remain in this state. This electron must be promoted to the conduction band or to a valence exciton state involving the valence hole in the emission final state. The energy required for this electron promotion accounts for the additional energy shift in the spectator valence emission ener-

gy. In Table III, the promotion energy is computed as the difference between the measured shifts for the specular valence spectra and the exciton spectra: 1.2 and 0.9 eV for LiBr and LiCl, respectively.

Since the measured binding energies of the core excitons are 1.3 and 1.85 eV in LiBr and LiCl (Table II), these are the expected shifts for promoting the electron to the bottom of the conduction band. These values may be reduced by as much as the valence exciton binding energy in these materials, which are approximately 0.3 and 0.6 eV.³³ The LiBr promotion energy corresponds closely to the core-exciton binding energy; however, the LiCl value exhibits a sizable discrepancy, possibly due to the higher valence exciton binding energy in LiCl. The uncertainty of almost 0.5 eV in the core-exciton binding energies of Table II can also account for much of the discrepancy. Both the core- and valence-exciton binding energies are subject to large errors originating from uncertainty in the band gap. The uncertainties of the measured promotion energies listed in Table III are smaller by nearly a factor of three. Accurate core-exciton binding energies, derived from precise measurements of the band gaps, would present a useful upper limit on the promotion contribution to the spectator emission shift.

Having separated the phonon relaxation and promotion contributions to the spectator shifts, we find that the phonon relaxation itself does not change very much in going from normal to spectator valence emission. In LiBr the phonon relaxation is 1.0 eV in either case, and in LiCl, the relaxation drops slightly, from 1.2 to 1.0 eV. This absence of substantial change is surprising since the phonon coupling strength Σ_{ph} was anticipated to decrease for localized excitations because the exciton screens the hole charge as seen by the lattice ions. O'Brien *et al.*³ determined Σ_{ph} in certain oxide insulators for both localized and continuum excitations by measuring as a function of temperature the widths of excitonic and bulk-derived features in SXE and SXA spectra. In MgO they measured Σ_{ph} values of 0.5 eV and 1.5 to 2.1 eV for localized and continuum excitations, respectively.

The absence of a difference in the phonon relaxation shift between normal and spectator excitation may be interpreted by first assuming that the hole lifetime is not influenced by the presence of the exciton. Then the localized excitations exhibit partial relaxation, following the same arguments made above for the continuum excitations. For partial relaxation, when the full $2\Sigma_{\text{ph}}$ Stokes shift is not achieved, the shift may not be proportional to Σ_{ph} but may instead be fairly independent of this parameter. One may also consider the possibility that the hole lifetime τ is in fact influenced by the presence of the exciton, which simultaneously screens the hole from the valence electrons and provides new hole decay paths via

direct recombination mechanisms. The former screening effect can increase τ , thereby allowing more complete relaxation to take place. This would partially compensate any reduction in the excitonic relaxation shift due to a lowering of Σ_{ph} . In any case, the 1.0 eV phonon relaxation shifts measured for localized Li *K* excitations in LiBr and LiCl represent a lower limit on the $2\Sigma_{\text{ph}}$ values for these localized excitations.

IV. CONCLUSIONS

The excitation and emission spectra of LiBr and LiCl have been measured around the Li *K* edge. Energy positions of the Li *K* exciton and Li *K* valence emission features were carefully quantified, and offsets relative to excitation-derived energies were analyzed and interpreted in terms of phonon relaxation. The Li *K* valence emission spectra for localized excitations were also shifted by the energy required to promote the localized electron when the core hole is annihilated. The comparison of phonon relaxation shifts for normal Li *K* excitations to estimated values of the complete $2\Sigma_{\text{ph}}$ suggests that partial relaxation takes place. The occurrence of partial relaxation for normal excitations is plausible when values of the hole lifetime and phonon relaxation time are compared. The relaxation shifts are found not to change substantially for spectator Li *K* excitations, indicating that Stokes shifts for partial relaxation are not proportional to Σ_{ph} . The phonon relaxation shift for the normal Br $M_{4,5}$ excitation in LiBr was also briefly analyzed. The strong valence charge transfer from Li to Br in this ionic compound contributes to a lowering of the Br excitation lifetime and subsequent reduction of the phonon relaxation. Overall, these various Stokes shifts provide a second approach to characterizing alkali-halide phonon coupling, which heretofore had been examined through phonon broadening of core-level and excitation spectra. These shifts yield further insight into the role of excitonic screening and chemical valence-charge-density effects in both the degree of phonon coupling and the balance between the phonon relaxation and excitation decay rates.

ACKNOWLEDGMENTS

We are grateful to S. E. Schnatterly, Honghong Wang, and Bernd Crasemann for helpful discussions. This research was supported by National Science Foundation Grant No. DMR-8715430 and by a Science Alliance Center for Excellence Grant from the University of Tennessee. The National Synchrotron Light Source is supported by DOE through Contract No. DE-AC02-CH00016.

*Present address: Physics Department, Brooklyn College of the City University of New York, Brooklyn, NY 11210.

¹W. L. O'Brien, J. Jia, Q.-Y. Dong, T. A. Callcott, K. E. Miyano, D. L. Ederer, D. R. Mueller, and C.-C. Kao, *Phys.*

Rev. B **47**, 140 (1993).

²W. L. O'Brien, J. Jia, Q.-Y. Dong, T. A. Callcott, K. E. Miyano, D. L. Ederer, D. R. Mueller, and C.-C. Kao, *Phys. Rev. Lett.* **70**, 238 (1993).

- ³W. L. O'Brien, J. Jia, Q.-Y. Dong, T. A. Callcott, D. R. Mueller, and D. L. Ederer, *Phys. Rev. B* **45**, 3882 (1992).
- ⁴A. Mansour and S. E. Schnatterly, *Phys. Rev. Lett.* **59**, 567 (1987).
- ⁵T. A. Callcott, E. T. Arakawa, and D. L. Ederer, *Phys. Rev. B* **16**, 5185 (1977).
- ⁶T. A. Callcott, E. T. Arakawa, and D. L. Ederer, *Phys. Rev. B* **18**, 6622 (1978).
- ⁷D. B. Fitchen, in *Physics of Color Centers*, edited by W. B. Fowler (Academic, New York, 1968), p. 293.
- ⁸C.-O. Almbladh, *Phys. Rev. B* **16**, 4343 (1977).
- ⁹G. D. Mahan, *Phys. Rev. B* **15**, 4587 (1977).
- ¹⁰R. Haensel, C. Kunz, and B. Sonntag, *Phys. Rev. Lett.* **20**, 262 (1968).
- ¹¹S. T. Pantelides, *Phys. Rev. B* **11**, 2391 (1975).
- ¹²References to numerous other SXA measurements from alkali halides are contained at the end of Ref. 11.
- ¹³T. A. Callcott, K. L. Tsang, C. H. Zhang, D. L. Ederer, and E. T. Arakawa, *Rev. Sci. Instrum.* **57**, 2680 (1986).
- ¹⁴T. A. Callcott, W. L. O'Brien, J. J. Jia, Q.-Y. Dong, D. L. Ederer, R. N. Watts, and D. R. Mueller, *Nucl. Instrum. Methods Phys. Res. A* **319**, 128 (1992).
- ¹⁵Pauling's electronegativities for the series F, Cl, Br are 4.0, 3.0 and 2.8. See L. Pauling, *The Nature of the Chemical Bond* (Cornell University Press, Ithaca, NY, 1960), p. 63.
- ¹⁶A. A. Maiste, A. M.-É Saar, and M. A. Élango, *Fiz. Tverd. Tela (Leningrad)* **16**, 1720 (1974) [*Sov. Phys. Solid State* **16**, 1118 (1974)].
- ¹⁷E. T. Arakawa and M. W. Williams, *Phys. Rev. Lett.* **36**, 333 (1976).
- ¹⁸O. Aita, K. Tsutsumi, K. Ichikawa, M. Kamada, and M. Okusawa, *Phys. Rev. B* **23**, 5676 (1981).
- ¹⁹K. L. Tsang, C. H. Zhang, T. A. Callcott, E. T. Arakawa, and D. L. Ederer, *Phys. Rev. B* **35**, 8374 (1987).
- ²⁰P. J. Feibelman and M. L. Knotek, *Phys. Rev. B* **18**, 6531 (1978).
- ²¹S. P. Kowalczyk, F. R. McFeely, L. Ley, R. A. Pollak, and D. A. Shirley, *Phys. Rev. B* **9**, 3573 (1974).
- ²²R. T. Poole, J. G. Jenkin, R. C. G. Leckey, and J. Liesegang, *Chem. Phys. Lett.* **22**, 101 (1973).
- ²³R. T. Poole, R. C. G. Leckey, J. G. Jenkin, and J. Liesegang, *Chem. Phys. Lett.* **31**, 308 (1975).
- ²⁴L. I. Johansson and S. B. M. Hagström, *Phys. Scr.* **14**, 55 (1976).
- ²⁵K. Ichikawa, M. Kamada, O. Aita, and K. Tsutsumi, *Phys. Rev. B* **32**, 8293 (1985).
- ²⁶W. L. O'Brien, J. Jian, Q.-Y. Dong, T. A. Callcott, J.-E. Rubensson, D. L. Mueller, and D. L. Ederer, *Phys. Rev. B* **44**, 1013 (1991).
- ²⁷The spectral features in Arakawa and Williams (Ref. 17) are presented on a logarithmic scale, which makes these features appear even broader than specified.
- ²⁸We used a background function that rises in proportion to the integrated intensity of the photoemission peak (integrated toward more negative binding energy) in order to account for the asymmetry in the photoemission background. The asymmetry arises in this case from contributions of the photoexcited valence electrons to the inelastically-scattered-electron tail. See D. A. Shirley, *Phys. Rev. B* **5**, 4709 (1972).
- ²⁹M. K. Wagner, J. C. Hansen, R. deSouza-Machado, S. Liang, J. G. Tobin, M. G. Mason, S. Brandt, Y. T. Tan, A.-B. Yang, and F. C. Brown, *Phys. Rev. B* **43**, 6405 (1991).
- ³⁰D. R. Mueller, J. Wallace, D. L. Ederer, J. J. Jia, W. L. O'Brien, Q.-Y. Dong, and T. A. Callcott, *Phys. Rev. B* **46**, 11069 (1992).
- ³¹F. C. Brown, C. Gähwiller, A. B. Kunz, and N. O. Lipari, *Phys. Rev. Lett.* **25**, 927 (1970).
- ³²A. B. Kunz and N. O. Lipari, *J. Phys. Chem. Solids* **32**, 1141 (1971).
- ³³G. Baldini and B. Bosacchi, *Phys. Status Solidi* **38**, 325 (1970).
- ³⁴The values given for the gap are based on the optical reflectivity measurements of Baldini and Bosacchi (Ref. 33) and are the commonly quoted values in the literature. In fact, however, the thresholds for band-gap excitations are not straightforward to extract from such reflectivity data because of valence excitonic structures preceding the thresholds. A second source of error for the band gaps is the fact that the reflectivity data of Baldini and Bosacchi were recorded at 55 K, whereas the room-temperature gaps are the relevant values for the present analysis. Haensel, Kunz, and Sonntag (Ref. 10) observed a 0.2 eV shift to higher energy for the Li K absorption spectrum of LiF when they cooled their sample from room to liquid nitrogen temperature, a manifestation of band-gap widening. The appropriate gaps for LiBr and LiCl at room temperature may thus be 0.2 eV or so smaller than listed.
- ³⁵K. Ichikawa, O. Aita, M. Kamada, and K. Tsutsumi, *Phys. Rev. B* **43**, 5063 (1991).
- ³⁶A. Mansour and S. E. Schnatterly, *Phys. Rev. B* **36**, 9234 (1987).
- ³⁷There also appears to be a shoulder in the C K exciton emission from diamond as measured by Y. Ma, N. Wassdahl, P. Skytt, J. Guo, J. Nordgren, P. D. Johnson, J. -E. Rubensson, T. Boske, W. Eberhardt, and S. D. Kevan, *Phys. Rev. Lett.* **69**, 2598 (1992). However, these authors do not focus on this aspect of the data.
- ³⁸J. Barth, C. Kunz, and T. M. Zimkina, *Solid State Commun.* **36**, 453 (1980).
- ³⁹A later photon-excited study of the boron compounds (Ref. 2) reported that the emission shoulder appears for a lower excitation energy than the main emission peak, thus calling the phonon ringing interpretation into question. However, since the main exciton peak in the B K emission overlaps the energy range of strong absorption in the boron compounds, it has been countered that the initial appearance of only the low-energy component may be a manifestation of self-absorption [S. E. Schnatterly (private communication)].
- ⁴⁰J. R. Fields, P. C. Gibbons, and S. E. Schnatterly, *Phys. Rev. Lett.* **38**, 430 (1977).
- ⁴¹A. Zunger and A. J. Freeman, *Phys. Rev. B* **16**, 2901 (1977).
- ⁴²C. E. Moore, *Atomic Energy Levels*, Natl. Bur. Stand. (U.S.) Circ. No. 467 (U.S. GPO, Washington, D.C., 1949), Vol. I, p. 10.
- ⁴³K. A. Jackson and M. R. Pederson, *Phys. Rev. Lett.* **67**, 2521 (1991).
- ⁴⁴The difference in instrumental broadening between the photoemission and SXE spectra, 1.3 versus 0.16 eV, leads to only a small difference when added quadratically to the full intrinsic width of the valence-band spectra, but this difference was nonetheless taken into account in the alignment procedure of Figs. 2, 3, and 5.
- ⁴⁵P. H. Citrin, P. Eisenberger, and D. R. Hamann, *Phys. Rev. Lett.* **33**, 965 (1974).
- ⁴⁶G. D. Mahan, *Phys. Rev. B* **21**, 4791 (1980).
- ⁴⁷D. Cubicciotti, *J. Chem. Phys.* **31**, 1646 (1959).
- ⁴⁸J. R. Tessman, A. H. Kahn, and W. Shockley, *Phys. Rev.* **92**, 890 (1953).
- ⁴⁹R. P. Lowndes, *Phys. Lett.* **21**, 26 (1966).

⁵⁰S. Haussühl, *Z. Naturforsch. Teil A* **12**, 445 (1957).

⁵¹G. Dolling, H. G. Smith, R. Nicklow, P. R. Vijayaraghavan, and M. K. Wilkinson, *Phys. Rev.* **168**, 970 (1968).

⁵²C. Sanjeeviraja, K. Kesavasamy, N. Krishnamurthy, and S. K.

Mohanlal, *J. Phys. Chem. Solids* **45**, 651 (1984).

⁵³Y. Baer, P. H. Citrin, and G. K. Wertheim, *Phys. Rev. Lett.* **37**, 49 (1976).

⁵⁴E. J. McGuire, *Phys. Rev. A* **5**, 1043 (1972).

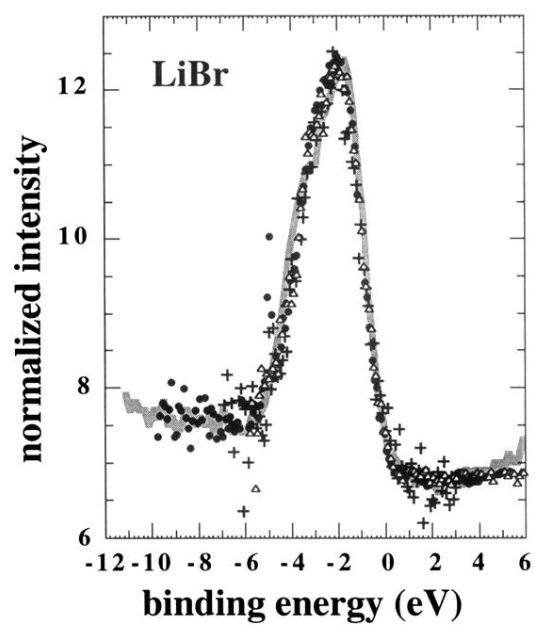


FIG. 2. Li *K* valence emission spectra from LiBr taken with excitation energies at 72.3 eV (closed circles), 67.5 eV (open triangles), and 59.7 eV (crosses) are superimposed on a valence photoemission spectrum from Ref. 24 (solid gray line) as described in the text.

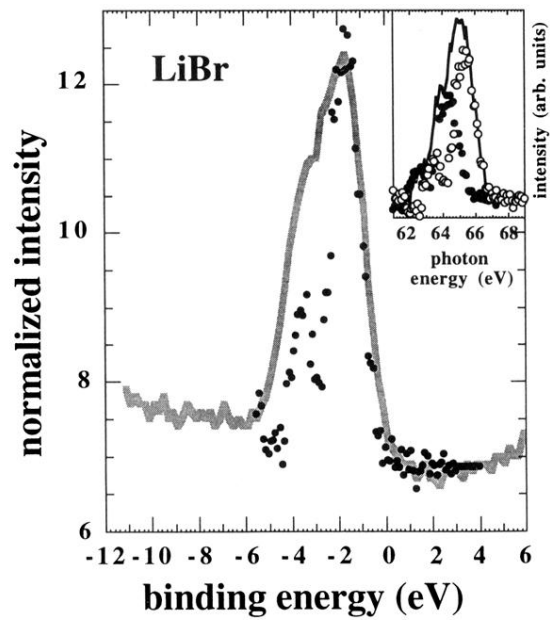


FIG. 3. A Br M_5 valence emission spectrum from LiBr taken with an excitation energy of 79.0 eV is superimposed on a valence photoemission spectrum from Ref. 24 (solid gray line) as described in the text. In the inset the decomposition of the Br $M_{4,5}$ valence emission spectrum into its M_4 (open circles) and M_5 (closed circles) components is shown.

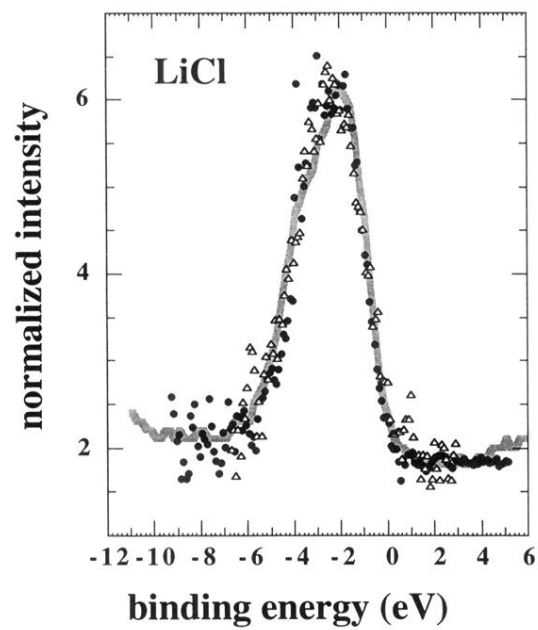


FIG. 5. Li *K* valence emission spectra from LiCl taken with excitation energies of 72.3 eV (closed circles) and 60.4 eV (open triangles) are superimposed on a valence photoemission spectrum from Ref. 24 (solid gray line) as described in the text.